Supplementary Information

Long-term persistency of a strong non-dipole field in the South Atlantic

Wellington P. de Oliveira[1], Gelvam A. Hartmann[1], Filipe Terra-Nova[2], Natália G. Pasqualon[3,4], Jairo F. Savian[4], Evandro F. Lima[4], Fernando R. da Luz[4], and Ricardo I. F. Trindade[5]

[1]Instituto de Geociências, Universidade Estadual de Campinas, 13083-855, Campinas, Brazil.
[2]Nantes Université, Univ Angers, Le Mans Université, CNRS, Laboratoire de Planétologie et Géosciences, LPG UMR 6112, 44000 Nantes, France.
[3]Department of Earth and Planetary Sciences, University of Hawai'i at Manoa, Honolulu, HI 96822, USA.
[4]Instituto de Geociências, Universidade Federal do Rio Grande do Sul, 91501-970, Porto Alegre, RS, Brazil.
[5]Instituto de Astronomia, Geofísica e Ciências Atmosféricas, Universidade de São Paulo, 05508-900, São Paulo, SP, Brazil.

Contents of this file

Supplementary Text

1 Geological setting of Trindade Island

The volcanic island of Trindade and the archipelago of Martin Vaz represent the emerged portions of the submarine chain Vitória-Trindade Ridge (VTR, Fig. 1). Trindade Island is located about 1260 km east of the Brazilian coast (20°30' S; 29°22' W) in the South Atlantic Ocean, and its origin is related to the upwelling of mantle plume material beneath the South American Plate since the Tertiary[1]. Studies[2–5] suggest that the submarine volcanic chain shares isotopic similarities with the alkaline continental magmatism seen in the Alto Parnaíba and Poxoréu Provinces (∼85 Ma), as well as the Abrolhos shelf (∼40-50 Ma)[3,4,6,7].

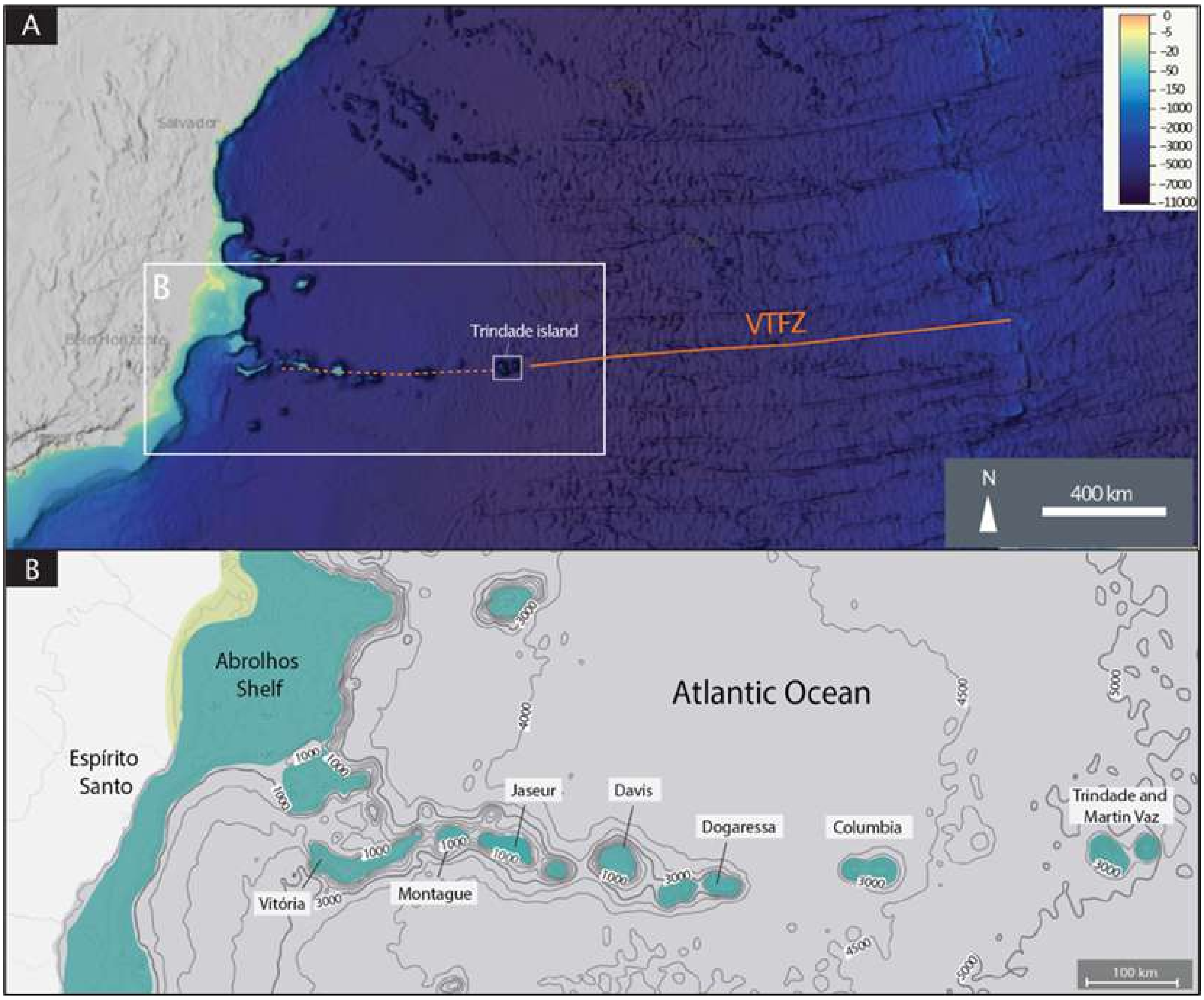

Supplementary Figure 1: **Geographical area of Trindade Island.** (a) Digital elevation model color shaded relief obtained from Bathymetric Data Viewer, National Oceanic and Atmospheric Administration (NOAA), highlighting the Vitória-Trindade Fracture Zone (VTFZ; indicated by red lines). Inset panel reprinted from[8], Copyright (2020), with permission from Elsevier. b) Vitória-Trindade Ridge bathymetric contour from the continental margin up to Trindade and Martin Vaz.

Trindade Island main axis is oriented a NW-SE, with geological structures indicating a predominant NW orientation of σ_1 during its formation[8,9]. The volcanic activity on the island started with the formation of Trindade Complex at ∼3.9 million years ago (Ar/Ar)[10] and persisted until about 1.1 Ma (K/Ar)[11]. This phase involved a diverse range of pyroclastic deposits, including melanephelinites to phonolites, prominent phonolitic necks and plugs (Fig. 2a), and dykes of varied compositions (Fig. 2b), such as olivine and clinopyroxene melanephelinites, monchiquites, and analcime basanites.

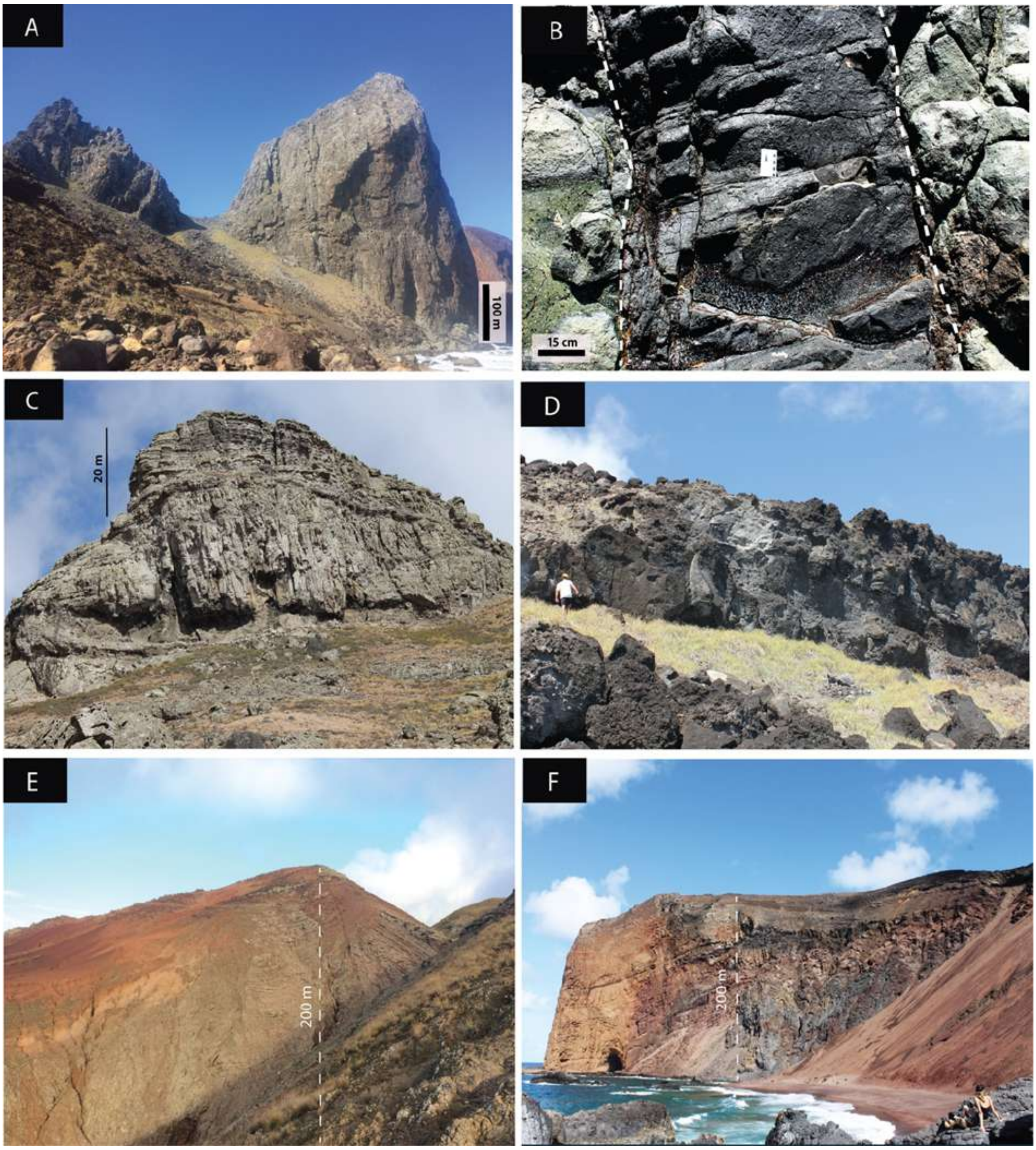

Supplementary Figure 2: **Field photographs of the geological units of Trindade Island.** a) Trindade Complex phonolitic neck; b) Trindade Complex melanephelinitic dyke; c) Interspersed lava flows and pyroclastic rocks from Desejado Formation; d) A'a lava flows from Valado Formation; e) Morro Vermelho Formation scoria cone; f) Paredao Volcano scoria cone.

Subsequently, the Desejado Formation volcanism (2.6–1.5 Ma; K/Ar)[11] overlaids the Trindade Complex. It primarily consists of phonolitic lava flows intermixed with lesser amounts of nephelinitic lava and pyroclastic rocks sharing similar compositions (Fig. 2c). The next episode of volcanism occurred during the Morro Vermelho Formation in the island's central-eastern area, characterized by melanephelinitic and ankaratritic lava flows followed by pyroclastic deposits (Fig. 2e). Initially dated around 0.27–0.17 Ma (K/Ar)[11], a recent assessment by Pasqualon et al.[12] suggests ages of 760-230 ka (Ar/Ar on whole rock) for this unit. The Valado Formation (Fig. 2d) formed at around 490 ka, and comprises melanephelinitic lava flows and minor proximal pyroclastic deposits.

The youngest geological unit on Trindade Island is the Paredão Volcano (Fig. 2f), with ages from 217-60 ka (Ar/Ar)[12]. This unit marks the final subaerial volcanic activity in Brazilian territory, wih lava flows visible at Tartarugas Beach and a pyroclastic cone concentrated in the southeastern part of the island. According to volcanological studies[1,13–15], the cone formed via a fire fountain process, rising approximately 200 meters above sea level. The volcanic products consist of lapilli-tuffs, bombs, blocks, agglomerated, and agglutinated materials from nephelinitic, basanitic, and tephritic lava.

2 Sampling

We conducted a fieldwork during July 2017 for paleodirectional analysis on Trindade Island. This island is located in a remote region of the South Atlantic Ocean and access to the targets was only possible with the support of the Brazilian navy. Due to the rugged topography, a collection of 160 rock sample cores were limited to 17 paleomagnetic sites from four geological formations within the study area (see Fig. 3 and Fig.1 in the main article). Among these sites, 8 were sampled in Trindade Complex of which seven correspond phonolitic necks (TR12, TR13, TR15A, TR16, TR17, TR18, and TR19), and one melanephelinitic dyke (TR15B). The remaining 9 sites are composed of olivine melanephelinitic to a'a flows for Morro Vermelho (TR06, TR07, TR08, and TR09), Valado (TR01A, TR01B and TR14) and Paredão Volcano (TR10 and TR11) formations. Around 10 core samples (2.5 cm in diameter and $\sim$10 cm in length) were collected at each site through a portable gasoline powered rock drill and oriented with a magnetic compass (Brunton) and when possible a sun compass was used. Site locations were acquired using a portable global positioning system device.

Supplementary Figure 3: **Images of paleomagnetic sites.** Images of some sampled sites (TR12, TR13, TR14, TR15, TR16, TR18) with core sample drill holes. TR = Trindade.

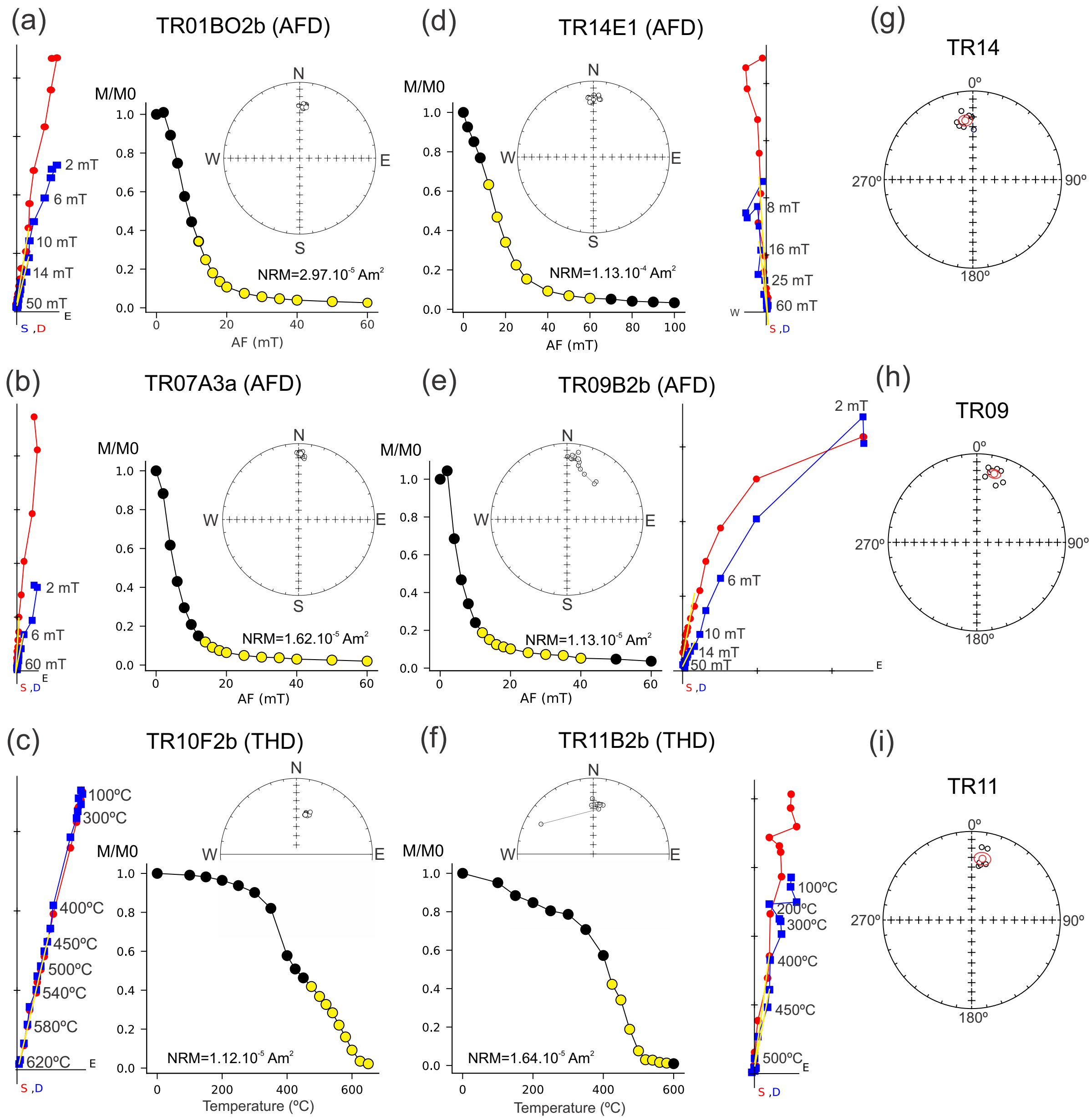

Supplementary Figure 4: **Graphical representation of the measurements obtained.** (a-f) Zidjerveld[16] diagrams from the alternating field (AFD) and thermal (THD) demagnetization resuls, together with the stereographic projections and normalized NRM intensity curves for representative samples from Trindade Island (TR). Specimen ChRM directions were determined by the best-fit lines indicated by the yellow circles. (g-i) Stereographic projections with the ChRM directions used to calculate the site-mean directions (red circles). NRM = natural remanent magnetization; ChRM = characteristic remanent magnetization. Source data are provided as a Source Data file.

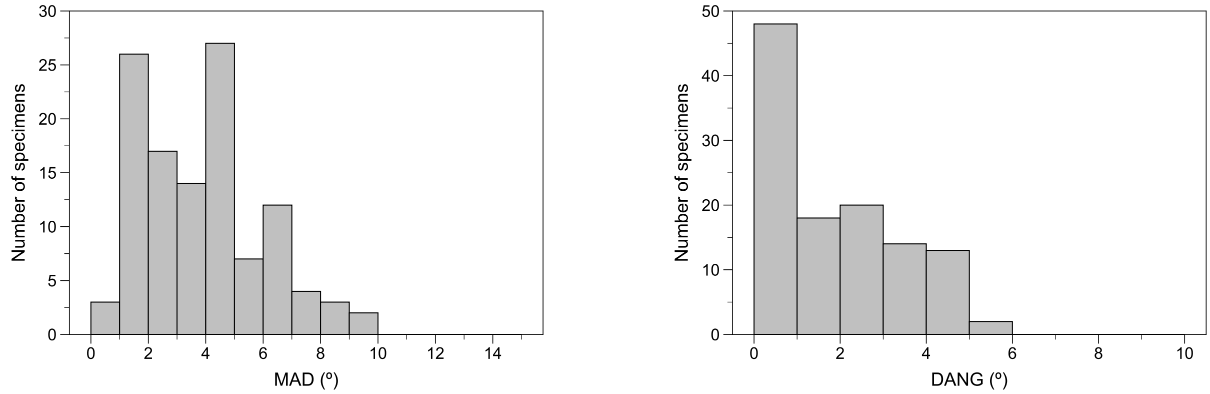

Supplementary Figure 5: **Specimen-level direction statistics.** Distributions of (a) MAD and (b) DANG estimates. MAD = maximum angular deviation; DANG = deviation angle.

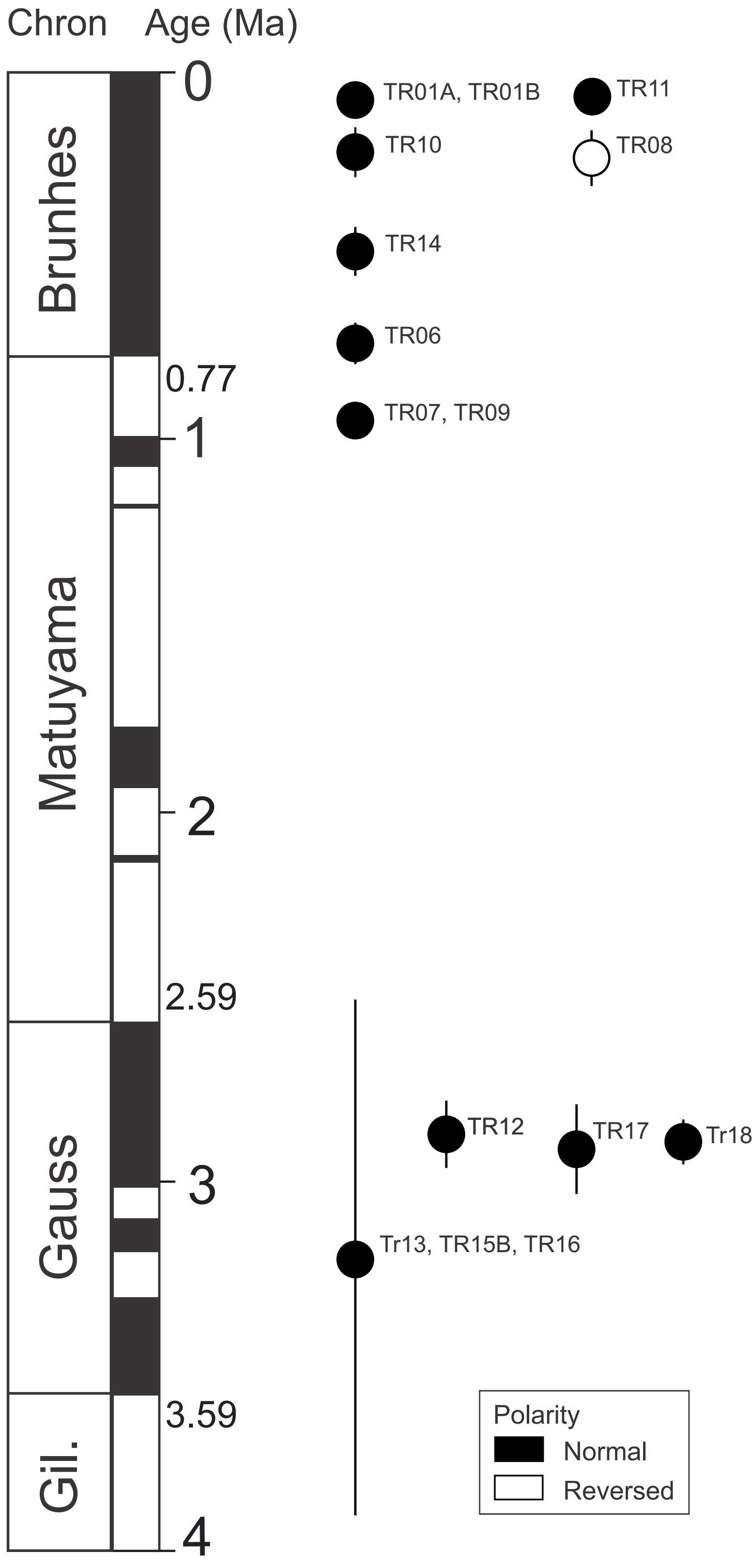

Supplementary Figure 6: **Comparison between the magnetic polarity of the site-mean directions and the geomagnetic polarity time scale 2020 (GPTS2020)[17]**. The age uncertainties assigned to the paleomagnetic sites (Table S1) are shown by vertical lines. Normal (reversed) polarity sites are represented by closed (empty) circles. Gil. = Gilbert chron.

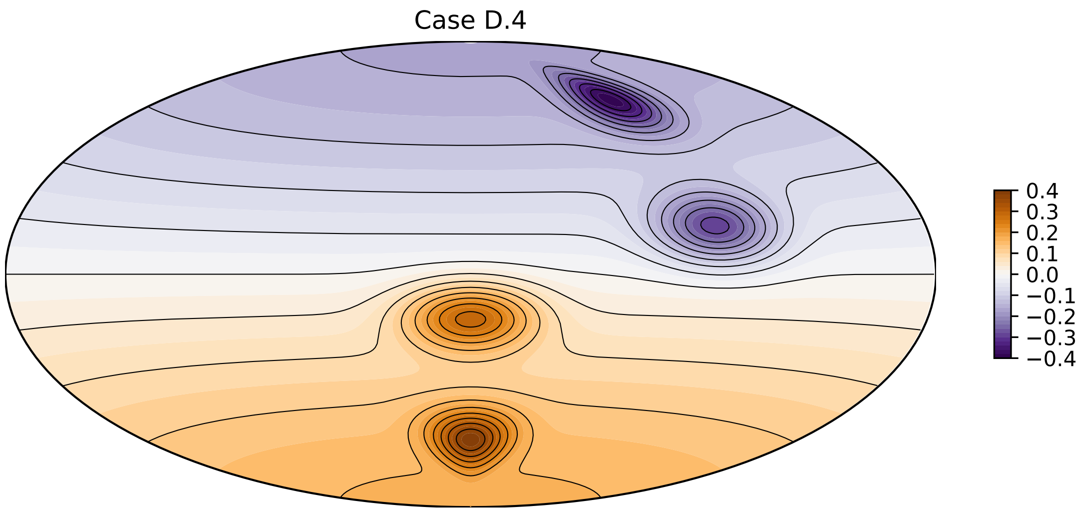

Supplementary Figure 7: **Map of the radial magnetic field at the core-mantle boundary.** Synthetic model for case D.4

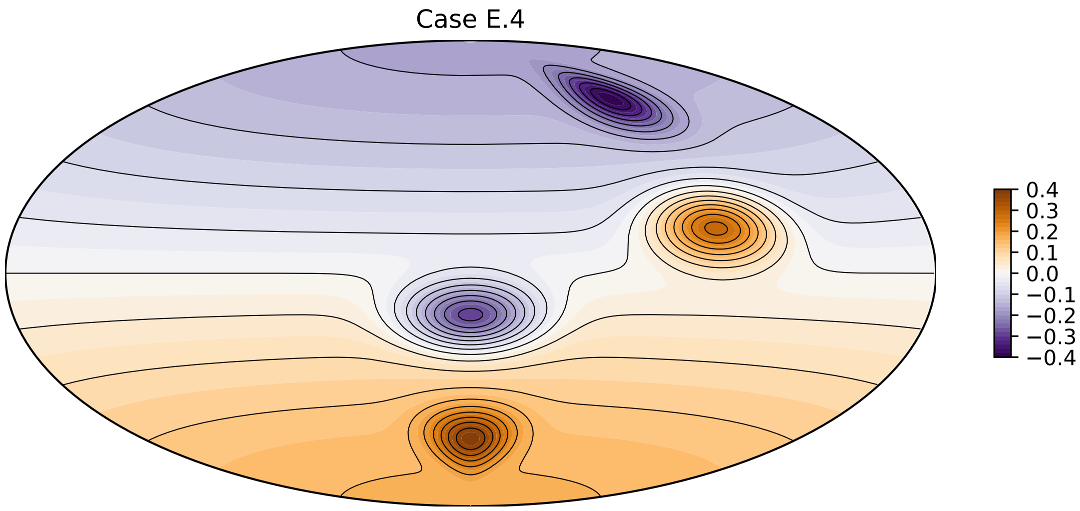

Supplementary Figure 8: **Map of the radial magnetic field at the core-mantle boundary.** Synthetic model for case E.4

Supplementary Table 1: Site-mean directions from Trindade Island.

Site	Slat (°N)	Slon (°E)	Slat* (°N)	Slon* (°E)	n	Demag	Dec (°)	Inc (°)	k	α_{95} (°)	VGP lat (°N)	VGP lon (°E)	Pol	Age (Ma)	Ref
TR01A	-20.50164	330.67936	-20.50120	330.65790	13	AF + Th	35.5	-49.6	128	3.7	56.6	85.2	N	0.077 ± 0.12	1
TR01B	-20.50128	330.67914	-20.50080	330.65768	11	AF + Th	12.3	-37.0	86	5.0	78.5	63.5	N	0.077 ± 0.12	1
TR06[a]	-20.51019	330.68908	-20.57803	330.69333	4	Th	46.7	-3.4	13	26.1	40.7	44.4	N	0.760 ± 0.078	1
TR07	-20.50837	330.68996	-20.57621	330.69421	7	AF	355.2	-15.0	84	6.6	76.2	310.3	N	0.9-1.0	1
TR08	-20.51089	330.68877	-20.52594	330.67314	7	AF	176.0	19.2	87	6.5	-78.7	130.2	R	0.232 ± 0.076	1
TR09	-20.50816	330.69078	-20.57600	330.69503	9	AF	14.2	-21.2	106	5.0	73.3	27.7	N	0.9-1.0	1
TR10	-20.51781	330.69822	-20.53136	330.68203	7	AF + Th	8.1	-45.5	120	5.5	80.2	103.2	N	0.217 ± 0.068	1
TR11	-20.51911	330.70094	-20.51757	330.67907	7	AF + Th	10.0	-30.4	83	6.7	79.6	38.6	N	0.066 ± 0.024	1
TR12	-20.51628	330.69445	-20.79407	330.77775	10	AF + Th	344.7	-45.1	161	3.8	74.8	215.2	N	2.86 ± 0.09	2
TR13	-20.51593	330.69324	-20.82772	330.78934	5	AF	337.4	-54.6	151	6.3	65.6	200.2	N	2.5-3.9	2
TR14	-20.50228	330.67953	-20.54292	330.67354	8	AF	352.7	-33.2	96	5.7	82.7	258.8	N	0.488 ± 0.067	1
TR15A	-20.49044	330.66692	-20.80221	330.76298	-	AF + Th	-	-	-	-	-	-	-	2.5-3.9	2
TR15B	-20.49044	330.66692	-20.80221	330.76298	7	AF + Th	7.7	-43.2	57	8.1	81.7	93.8	N	2.5-3.9	2
TR16[a]	-20.48922	330.66508	-20.80099	330.76114	5	AF + Th	8.9	-21.8	37	12.7	77.2	14.1	N	2.5-3.9	2
TR17	-20.51140	330.68544	-20.79319	330.77023	10	AF	320.4	-62.3	103	4.8	50.0	196.7	N	2.90 ± 0.12	3
TR18	-20.51692	330.68992	-20.79671	330.77397	9	AF + Th	22.3	-12.4	159	4.2	64.0	30.0	N	2.88 ± 0.06	2
TR19	-20.52007	330.69181	-20.80986	330.77962	-	AF + Th	-	-	-	-	-	-	-	2.98 ± 0.07	2

Slat and Slon refer site latitude and longitude; Slat* and Slon* are the paleolocations after implementing plate movement corrections; n is amount of specimens; Demag corresponds to the demagnetization technique employed: alternating-field (AF) or thermal (Th) treatments; Dec and Inc are declination and and inclination of site-level direction; k is the Fisher[18] precision parameter; α_{95} is the radius of 95% confidence cone; VGP lat and VGP lon refer the latitude and longitude of the virtual geomagnetic pole; Pol denotes the geomagnetic polarity: normal (N) and reversed (R); and Reference (Ref): 1. Pasqualon et al.[12]; 2. Pires et al.[10]; 3. Cordani[11].

[a]Site-mean directions that do not satisfy the selection criterion mentioned in the main article.

Supplementary Table 2: Mean directions from Trindade Island.

Site groups	Paleolat (°N)	Paleolon (°E)	N	D (°)	I (°)	α_{95} (°)	k	Plat (°N)	Plon (°E)	A_{95} (°)	K	S_B (°)	S_{Bl} (°)	S_B^u (°)	ΔI (°)	ΔI_{lo} (°)	ΔI^{up} (°)
All data	-20.66	330.72	15	7.1	-34.5	11.7	11.7	84.5	60.4	11.1	12.8	22.8	14.1	28.7	2.5	-6.0	11.2
$n \geq 5$, $k \geq 50$	-20.64	330.72	13	3.2	-37.3	11.1	14.9	87.3	100.0	10.9	15.6	20.6	13.9	26.1	-0.3	-9.2	8.6

Paleolat and Paleolon correspond to the mean site paleolatitude and paleolongitude; N is the number of sites; D and I refer the mean declination and inclination; k and α_{95} are the Fisher[18] precision parameter and 95% confidence cone about mean direction; Plat and Plon are the coordinates of the paleopole; K and A_{95} are the Fisher precision parameter and 95% confidence cone about paleopole; S_B is the between-site VGP dispersion with lower (S_{Bl}) and upper (S_B^u) bootstrap 95% confidence limits; ΔI is the inclination anomaly with lower (ΔI_{lo}) and upper (ΔI^{up}) bootstrap 95% confidence limits. VGP = virtual geomagnetic pole.

Supplementary References

1. Almeida, F. F. M. Ilhas oceânicas brasileiras e suas relações com a tectônica atlântica. *Terrœ Didatica* **2,** 3–18 (2006).
2. O'Connor, J. M. & Duncan, R. A. Evolution of the Walvis Ridge Rio Grande Rise hot spot system: Implications for African and South American plate motions over plumes. *Journal of Geophysical Research: Solid Earth* **95,** 17475–17502 (1990).
3. Gibson, S. A., Thompson, R. N., Leonardos, O. H., Dickin, A. P. & Mitchell, J. G. The Late Cretaceous impact of the Trindade mantle plume: Evidence from large-volume, mafic, potassic magmatism in SE Brazil. *Journal of Petrology* **36,** 189–229 (1995).
4. Gibson, S. A., Thompson, R. N., Weska, R. K., Dickin, A. P. & Leonardos, O. H. Late Cretaceous rift-related upwelling and melting of the Trindade starting mantle plume head beneath western Brazil. *Contributions to Mineralogy and Petrology* **126,** 303–314 (1997).
5. Siebel, W. *et al.* Trindade and Martín Vaz Islands, South Atlantic: Isotopic (Sr, Nd, Pb) and trace element constraints on plume related magmatism. *Journal of South American Earth Sciences* **13,** 79–103 (2000).
6. Fodar, R. V., Mukasa, S. B., Gomes, C. B. & Cordani, U. G. Ti-rich Eocene basaltic rocks, Abrolhos platform, offshore Brazil, 18º S: Petrology with respect to South Atlantic magmatism. *Journal of Petrology* **30,** 763–786 (1989).
7. Fodor, R. V. & Hanan, B. B. Geochemical evidence for the Trindade hotspot trace: Columbia seamount ankaramite. *Lithos* **51,** 293–304 (2000).
8. Pasqualon, N. G. *et al.* Emplacement dynamics of alkaline volcanic and subvolcanic rocks in Trindade Island, Brazil. *Journal of Volcanology and Geothermal Research* **406,** 1–20 (2020).
9. Ferrari, A. L. & Riccomini, C. Campo de esforços Plio-Pleistocênico na Ilha de Trindade (Oceano Atlântico Sul, Brasil) e sua relação com a tectônica regional. *Revista Brasileira de Geociências* **29,** 195–202 (1999).
10. Pires, G. L. C. *et al.* New ^{40}Ar/^{39}Ar ages and revised ^{40}K/^{40}Ar* data from nephelinitic–phonolitic volcanic successions of the Trindade Island (South Atlantic Ocean). *Journal of Volcanology and Geothermal Research* **327,** 531–538 (2016).
11. Cordani, U. G. Idade do vulcanismo no oceano Atlântico Sul. *IAG Boletim* **1,** 09–75 (1970).
12. Pasqualon, N. G. *et al.* New volcanological, ^{40}Ar/^{39}Ar dating and paleomagnetic record from Trindade Island and stratigraphic implications. *Quaternary Geochronology* **81,** 101518 (2024).
13. Almeida, F. F. M. *Geologia e petrologia da Ilha da Trindade* (Serviço Gráfico do Instituto Brasileiro de Geografia e Estatística, 1961).
14. Almeida, F. F. M. Ilha de Trindade, registro de vulcanismo cenozoico no Atlântico Sul. *Sítios geológicos e paleontológicos do Brasil,* 369–377 (2002).
15. Pasqualon, N. G., de Lima, E. F., dos Santos Scherer, C. M., Rossetti, L. d. M. M. & da Luz, F. R. Lithofacies association and stratigraphy of the Paredão Volcano, Trindade Island, Brazil. *Journal of Volcanology and Geothermal Research* **380,** 48–63 (2019).

16. Zijderveld, J. D. A. in Colison, D. W. *Methods in Paleomagnetism* 254–286 (Amsterdam: Elsevier, 1967).

17. Ogg, J. G. in *Geologic time scale 2020* 159–192 (Elsevier, 2020).

18. Fisher, R. A. Dispersion on a sphere. *Proc. R. Soc. Lond* **A217,** 295–305 (1953).